

# The Redshift Distribution of Type-Ia Supernovae: Constraints on Progenitors and Cosmic Star Formation History

Avishay Gal-Yam<sup>1,2</sup> and Dan Maoz<sup>1</sup>

<sup>1</sup> School of Physics & Astronomy and Wise Observatory, Tel Aviv University, Tel Aviv 69978, Israel; avishay@wise.tau.ac.il

<sup>2</sup> Colton Fellow.

Accepted - . Received - ;

## ABSTRACT

We use the redshift distribution of type-Ia supernovae (SNe) discovered by the Supernova Cosmology Project to constrain the star formation history (SFH) of the Universe and SN Ia progenitor models. Given some of the recent determinations of the SFH, the observed SN Ia redshift distribution indicates a long ( $\gtrsim 1h^{-1}$  Gyr) mean delay time between the formation of a stellar population and the explosion of some of its members as SNe Ia. For example, if the Madau et al. (1998) SFH is assumed, the delay time  $\tau$  is constrained to be  $\tau \geq 1.7(\tau \geq 0.7)h^{-1}$  Gyr at the 95%(99%) confidence level (CL). SFHs that rise at high redshift, similar to those advocated by Lanzetta et al. (2002), are inconsistent with the data at the 95% CL unless  $\tau > 2.5h^{-1}$  Gyr. Long time delays disfavor progenitor models such as edge-lit detonation of a white dwarf accreting from a giant donor, and the carbon core ignition of a white dwarf passing the Chandrasekhar mass due to accretion from a subgiant. The SN Ia delay may be shorter, thereby relaxing some of these constraints, if the field star formation rate falls, between  $z = 1$  and the present, less sharply than implied, e.g., by the original Madau plot. We show that the discovery of larger samples of high- $z$  SNe Ia by forthcoming observational projects should yield strong constraints on the progenitor models and the SFH. In a companion paper, we demonstrate that if SNe Ia produce most of the iron in galaxy clusters, and the stars in clusters formed at  $z \sim 2$ , the SN Ia delay time must be *lower* than 2 Gyr. If so, then the Lanzetta et al. (2002) SFH will be ruled out by the data presented here.

**Key words:** galaxies: supernovae: general.

## 1 INTRODUCTION

The evolution of the SN rate over cosmic time is a key ingredient for understanding the chemical enrichment history of the Universe and the formation and properties of galaxies and clusters. Since the progenitors of core-collapse SNe are massive, short-lived stars, their cosmic rate evolution will closely follow the universal star formation history (SFH). On the other hand, the actual route that leads a white dwarf (WD) to explode as a SN Ia is still an open question (see, e.g., Yungelson & Livio 2000, and references therein).

The mechanism that leads to the explosions of SNe Ia likely involves a significant delay between the formation of the progenitor system and the explosion of the SN. The rate of SNe Ia at a given epoch is therefore expected to depend on the star formation rate up to several Gyr preceding that

epoch. Thus, the cosmic evolution of SN rates can be used to constrain both the global SFH, and the characteristic delay time between star formation and SN Ia explosion (e.g., Madau, Della Valle & Panagia 1998; hereafter MDP). Since competing SN Ia models predict different delay times, observational constraints on the delay can discriminate between some of the proposed scenarios for SN Ia progenitor systems.

During the last few years, SNe Ia have been used successfully as cosmological distance indicators (e.g., Riess et al. 1998,2001; Perlmutter et al. 1999; Tonry et al. 2003). Perhaps the main uncertainty that still plagues SN-Ia-based distance measurements is the possibility of evolution in SN Ia properties. The use of SNe Ia as distance estimators relies on the assumption that distant SNe Ia at redshifts as high as  $z = 1.7$  are similar to local events. In order to study this question from a theoretical perspective, we require knowl-

edge on the nature of the progenitor systems of SNe Ia. For any given scenario, it is possible to estimate the evolution of high- $z$  systems relative to local ones, e.g., as a result of metallicity or stellar-age effects. Determination of SN Ia delay times, with the resulting constraints on progenitor models, are therefore desirable.

Motivated by these questions, a number of authors have recently studied the evolution of SN rates. Most studies have combined models of the SFH with a recipe for the delay function of SNe Ia, and have calculated the expected evolution of SN rates, either per unit comoving volume, or per unit stellar luminosity (e.g. Jørgensen et al. 1997; Sadat et al. 1998; MDP; Ruiz-Lapuente & Canal 1998; Yungelson & Livio 1998; Kolatt & Bartelmann 1998). As measurements of SN Ia rates at high  $z$  have become available (Pain et al. 1997; 2002) attempts have been made to compare the observed rates with model predictions (e.g., MDP; Sadat et al. 1998; Kobayashi et al. 1998; Kobayashi, Tsujimoto, & Nomoto 2000; Pain et al. 2002; Calura & Matteucci 2003). However, no strong conclusions have been reached regarding the SFH or SN Ia progenitors.

All available measurements of SN rates beyond the local Universe (Pain et al. 1997; 2002; Hardin et al. 2000; Gal-Yam, Maoz, & Sharon 2002; Tonry et al. 2003) are based on SNe Ia in the redshift range  $z = 0 - 1$ . Due to the limited number of observed SNe Ia, these studies have distributed their samples into wide redshift bins. In Gal-Yam et al. (2002) we divided our sample into two redshift bins, with  $\langle z \rangle = 0.25$  and  $\langle z \rangle = 0.9$ . This binning caused no loss of information in our work, as the number of bins was comparable to the number of SNe (2–3). On the other hand, Pain et al. (1997; 2002) and Tonry et al. (2003) used only one bin, and calculated the SN rate at an average redshift,  $z \sim 0.5$ . In these cases, most of the redshift information is lost in the binning process.

This loss may be averted if, instead of deriving absolute rates from the observations, and comparing them to predicted rates, we begin with the predictions and fold them through the observational filters. We can then compare the prediction for a particular experiment with the unbinned observations. Specifically, we can test whether or not the unbinned distribution of SN redshifts in a particular survey is consistent with some model. Indeed, several authors have calculated such distributions (e.g., Dahlé & Fransson 1999, hereafter DF; Sullivan et al. 2000a). DF noted that these distributions can be used to constrain progenitor models. However, they concentrated on future, deep surveys with the *James Webb Space Telescope*, and did not attempt to constrain model parameters using existing SN data.

Pain et al. (1997, 2002) and Tonry et al. (2003) have calculated the expected redshift distributions of SNe in their respective surveys, and have compared them with the observed distributions as part of their derivation of SN rates. However, the SN redshift distributions calculated by Pain et al. and Tonry et al. are based on particular assumptions about the evolution of the SN Ia rate between  $z = 0$  and  $z \sim 1$ , which is assumed to be either constant (Tonry et al. 2003), or to vary as some power of the redshift (Pain et al. 2002). The comparison between the expected and observed SN Ia redshift distributions is used to find the best fitting rate evolution, and to derive the average SN Ia rate at the mean redshift ( $z \sim 0.5$  in both cases). Again, the in-

formation contained in the redshift distribution of SNe Ia at  $z = 0 - 1$  is lost in the averaging process. Both groups note that their data seem to indicate a slowly varying SN Ia rate in this redshift range. Tonry et al. conclude that, given that the slope of the SN Ia rate is shallower than that of some determinations of the SFH in this redshift range, the typical delay time between star formation and SN Ia explosion must be  $\sim 1$  Gyr.

In view of the fact that some models (e.g., MDP) predict strong evolution in the SN Ia rate at  $z = 0 - 1$ , in contrast with the trends seen by Pain et al. (2002) and Tonry et al. (2003), we have undertaken a more comprehensive investigation of the SN Ia redshift distribution in this range. As we will show below, existing data can already place interesting limits on the SFH and on the SN Ia characteristic delay time.

Throughout this paper, we assume a flat cosmology with  $\Omega_m = 0.3$  and  $\Omega_\Lambda = 0.7$ . We designate with  $h$  the Hubble parameter in units of  $100 \text{ km s}^{-1} \text{ Mpc}^{-1}$ .

## 2 CALCULATION OF THE SUPERNOVA REDSHIFT DISTRIBUTION

We begin by calculating  $N(z, R_{lim})$ , the redshift distribution of SNe visible in a region of sky at a given moment, to a limiting  $R$ -band magnitude  $R_{lim}$ . Throughout this paper, we assume that all apparent magnitudes are measured in the  $R$ -band. Our calculations can be applied to any other band, as long as all apparent magnitudes are measured in the same band. Then,

$$N(z, R_{lim}) = n(z) \times dV(z) \times T(z, R_{lim}) \quad , \quad (1)$$

where  $n(z)$  is the SN rate density, defined as the number of SNe per unit time per unit volume as a function of the redshift, and  $dV(z)$  is the volume between  $z$  and  $z + dz$  in that region of sky.  $T(z, R_{lim})$  is the effective visibility time of a SN at redshift  $z$ , given the detection efficiency as a function of magnitude (this is often referred to as the “control time”).  $T$  depends on  $z$  because SNe at higher  $z$  are fainter, and therefore can be detected for a shorter period above the limiting magnitude  $R_{lim}$ . The brightness of the SN in the chosen bandpass also depends on  $z$  since different parts of the SN spectrum are redshifted into the observed band for SNe at different redshifts.

The SN Ia rate density,  $n(z)$ , is a convolution of the star-formation history (SFH) with a “delay” or “transfer function”, which is the SN Ia rate vs time following a brief burst of star formation. The delay function accounts for the time span between star formation, through stellar evolution, the formation of WDs, and the final stage where a WD accretes material from (or spirals in and merges with) a binary companion (MDP; DF). We follow here the delay function parameterization given by MDP. The overall time delay includes the mass-dependent lifetime of the progenitor as a main-sequence star,  $\Delta t_{MS}$ . Once the progenitor has gone off the main-sequence and has become a WD, it has a probability  $\propto \exp(-\frac{\Delta t}{\tau})$  to explode as a SN Ia, where  $\Delta t$  is the time since the star left the main sequence. DF have proposed a simpler model, with a discrete delay time,  $\tau$ , which we further consider in section § 4.2. Since we will be interested solely in the redshift distribution of SNe, we will

ignore the normalization of  $n(z)$ . Integrating the explosion probabilities over the stellar initial mass function,  $dN/dm$ , and the past SFH,  $\Psi(t)$ , the SN rate density as a function of cosmic time is

$$n(t) \propto \int_0^t \Psi(t') dt' \times \int_{m_{\min}(t-t')}^{m_{\max}} \exp\left(-\frac{t-t'-\Delta t_{MS}}{\tau}\right) \frac{dN}{dm}(m) dm, \quad (2)$$

where,  $m_{\min}$  and  $m_{\max}$  are the minimum and maximum initial masses that will lead to the formation of a WD that explodes as a SN Ia. Following MDP, we adopt

$$m_{\min} = \max\left[3M_{\odot}, \left(\frac{t-t'}{10 \text{ Gyr}}\right)^{-0.4} M_{\odot}\right], \quad m_{\max} = 8M_{\odot},$$

and  $\frac{\Delta t_{MS}}{10 \text{ Gyr}} = \left(\frac{m}{M_{\odot}}\right)^{-2.5}$ . (3)

A Salpeter (1955) initial mass function (IMF),  $dN/dm \sim m^{-2.35}$ , is assumed. We convert  $n(t)$  to  $n(z)$  using the transformation between cosmic time and redshift,

$$\Delta t = \frac{1}{H_0} \int_{z_1}^{z_2} \frac{dz}{(1+z)[(1+z)^3 \Omega_m + \Omega_{\Lambda}]^{1/2}}. \quad (4)$$

The detailed form of the SFH,  $\Psi$ , is a much debated issue in recent years. Initial studies of the UV to IR luminosity density of star-forming galaxies (e.g., Lilly et al. 1996; Madau et al. 1996; Connolly et al. 1997, Madau, Pozzetti, & Dickinson, 1998) suggested that the SFH increases sharply between redshifts of zero and  $z \sim 1-2$ , and then decreases at higher  $z$ . However, this picture has been challenged. For instance, Steidel et al. (1999) argue for an almost-constant SFH at  $z \sim 1-4$ , while Lanzetta et. al. (2002) favor a monotonic increase in SFH out to  $z = 10$ . At lower redshifts, Cowie, Songaila, & Barger (1999) and Sullivan et al. (2000a) have found the SFH slope at  $z \sim 0-1$  to be quite shallow,  $\Psi(z) \sim (1+z)$ , but recent measurements by Hippelein et al. (2003) seem to confirm the sharp rise,  $\Psi \sim (1+z)^4$ , initially reported by Lilly et al. (1996).

To parameterise this range of possibilities for  $\Psi(z)$ , we represent the SFH by a broken power law, with  $\Psi(z) \sim (1+z)^{\alpha}$  at high  $z$ , and  $\Psi(z) \sim (1+z)^{\beta}$  at low  $z$ . These functions are joined smoothly at  $z = 1.2$ , using the prescription of Beuermann et al. (1999; see also Bersier et al. 2003),

$$\Psi(z) = \frac{2^{1/s} \times \Psi(1.2)}{\left[\left(\frac{2.2}{1+z}\right)^{\alpha \times s} + \left(\frac{2.2}{1+z}\right)^{\beta \times s}\right]^{1/s}}, \quad (5)$$

with  $s = 5$ . The high- $z$  index  $\alpha$  assumes values between  $\alpha = -2$ , which corresponds to the results of Madau et al. (1998), and  $\alpha = 2$ , which describes the work by Lanzetta et al. (2002). Similarly, the low- $z$  index  $\beta$  varies between  $\beta = 4$ , as advocated by Hippelein et al. (2003), and  $\beta = 1$ , tracing the results of Cowie et al. (1999)\*. Fig. 1a shows two examples of the SFH parameterization. With these ingredients, each model for the SN rate density  $n(z)$  is determined by three

\* In the case of  $\beta = 1$ , the Beuermann prescription causes the high- $z$  portion of the SFH function to remain somewhat affected by the low- $z$  index  $\beta$  even at redshifts much larger than  $z = 1.2$ . In that case, we therefore use a simple broken power law.

parameters - the typical delay time  $\tau$  and the two indices describing the SFH,  $\alpha$  and  $\beta$ . Fig. 1b shows two examples of SN Ia delay functions, and Fig. 1c shows two examples of  $n(z)$  for particular combinations of SFH and  $\tau$ .

For our chosen cosmology, the volume element is given by,

$$dV(z) \propto D_A^2 \times c \frac{dt}{dz} \propto \frac{[\int_0^z \chi dz']^2}{(1+z)^2} \times \frac{\chi}{(1+z)}, \quad (6)$$

where  $D_A$  is the angular diameter distance, and  $\chi$  is given by

$$\chi = \frac{1}{[\Omega_m(1+z')^3 + \Omega_{\Lambda}]^{1/2}}. \quad (7)$$

In the calculation of the effective visibility time  $T(z, R_{lim})$  we follow the procedures described in Gal-Yam et al. (2002). Briefly, assuming initially that SNe Ia are perfect standard candles with identical light curves, the peak magnitude of a SN at a given redshift is  $R_{peak}(z)$ , and the period it spends above some limiting magnitude  $R_{lim}$  can be easily determined. The efficiency of a survey,  $\eta$ , is generally a function of the apparent magnitude  $R$  (with  $R_{lim}$  defined by  $\eta(R_{lim}) = 0$ ), and is assumed to be independent of the SN redshift, i.e., the detection probability is the same for SNe with the same magnitudes but different redshifts. Weighting the time the SN spends above the detection limit by the relevant efficiency values, gives

$$T(z) = \int_0^{\infty} \eta[R(t, z)] dt, \quad (8)$$

where  $R(t, z)$  is the light curve of a SN Ia at redshift  $z$ , and  $\eta = 0$  when  $R(t) \geq R_{lim}$ . Note that cosmological time dilation will slow down the evolution of the light curves (e.g., Leibundgut et al. 1996, Goldhaber et al. 1997, Riess et al. 1997), and hence lengthen the visibility times of SNe Ia by  $(1+z)$ , but this is canceled out in the calculation of  $N(z)$  by the  $(1+z)$  reduction of the observed SN rate at redshift  $z$ .

The SN survey data whose redshift distribution we will model were obtained in the  $R$  band, and range in redshift from  $z = 0.361$  to  $z = 0.778$ . We require information on  $R(t)$  and  $R_{peak}(z)$  in order to calculate  $T(z)$ . To determine  $R_{peak}(z)$ , we fit a 3rd-order polynomial to the observed  $R$ -band peak magnitudes of high- $z$  SNe reported by Perlmutter et al. (1998, 1999). Note that no K-corrections are needed, as the input we require are the peak  $R$  magnitudes at all redshifts, and these do not have to be translated into rest frame  $B$  magnitudes, as done by the SCP for Hubble-diagram purposes. In terms of the light curves,  $R(t)$ , the observer-frame  $R$  band is a fair match for rest-frame  $B$  band in most of the redshift range we model. However, at the highest and lowest redshifts, rest-frame  $U$  and  $V$  wavelengths, respectively, dominate the observer-frame  $R$  band. Since the light curves of SNe Ia have slightly different forms in each band, we have constructed a set of  $z$ -dependent observer-frame light curves, by linearly interpolating between the appropriate rest-frame light curves. The template light curves were adapted from  $U$ ,  $B$  and  $V$  light curves, kindly supplied by B. Leibundgut, and supplemented with data points taken from Riess et al. (1999), which also give slightly better coverage of the pre-maximum period. Early  $U$ -band observations of SNe Ia are scarce, so we had to extrapolate the rest-frame  $U$ -band light

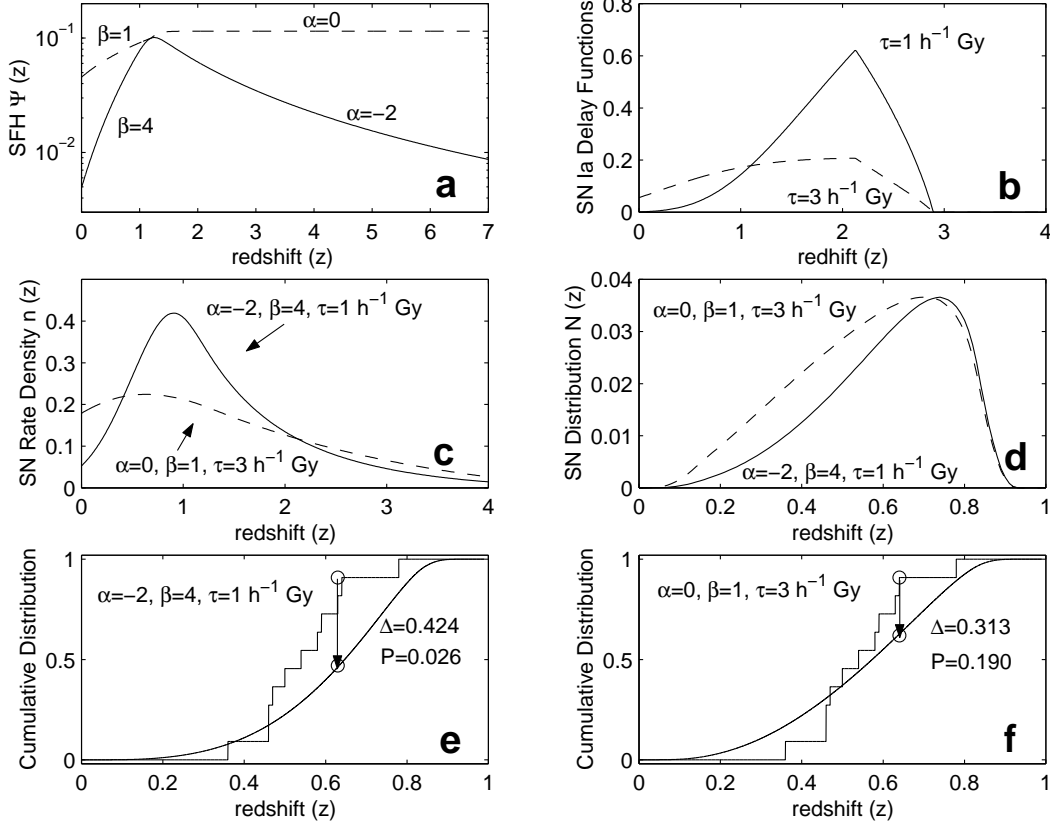


**Figure 1.** Illustration of the modeling and comparison to data. Panel a shows two examples of the SFH,  $\Psi(z)$  - a “Madau” SFH, with a peak at  $z = 1.2$  (solid curve), and a shallower model (dashed curve) reflecting the proposed modifications by Cowie et al. (1999) and Steidel et al. (1999). Panel b shows two examples of the expected SN Ia rate density following a brief burst of star formation. These delay functions are calculated using the MDP prescription, with characteristic exponential delay times of  $\tau = 1 h^{-1}$  Gyr (solid) and  $\tau = 3 h^{-1}$  Gyr (dashed). For display purposes, an arbitrary redshift of  $z = 3$  has been chosen for the burst of star formation. SFH models are convolved with a delay function, and the resulting SN rate densities  $n(z)$  for a “Madau” SFH with  $\tau = 1 h^{-1}$  Gyr (solid) and a “Cowie-Steidel” SFH with  $\tau = 3 h^{-1}$  Gyr (dashed) are shown in panel c. Panel d shows the predicted SN distributions,  $N(z)$ , for the models of panel c, in a survey with the same observational parameters of the SCP search described in § 3. KS tests show that the cumulative version of  $N(z)$  from a model combining a “Madau” SFH with a typical delay time of  $\tau = 1 h^{-1}$  Gyr (panel e) is ruled out by the data, while a model with “Cowie-Steidel” SFH and  $\tau = 3 h^{-1}$  Gyr is consistent with the data (panel f). Vertical axis units are arbitrary in panels a-d.

curve. However, this extrapolated curve is only relevant for high- $z$  SNe, which are invariably discovered close to the limiting magnitude. Therefore, the influence of the extrapolated part of the light curve, well below the peak magnitude, is negligible. The  $R_{peak}(z)$  curve and observer frame  $R$ -band light curves represent the properties of an average SN Ia.

In reality, the peak magnitudes and light curve shapes are not uniform. “Peculiar” SNe Ia are quite common in low- $z$  SN samples, but they are apparently absent from high- $z$  samples like the ones we consider (Li et al. 2001). One may worry that many SNe Ia of the “underluminous”, 1991bg-like, variety are missed at high  $z$  due to their lower luminosity, and we return to consider this possibility in section § 4.2. Even spectroscopically “normal” SNe Ia are not perfect standard candles, and exhibit an intrinsic scatter of 0.2–0.3 mag in peak luminosity (see Branch 1998, for a review). The peak magnitude of a SN Ia is correlated with the light-curve shape of the object, with brighter events having a slower rise to maximum followed by a slower decline (e.g., Phillips 1993; Phillips et al. 1999; Riess, Press, & Kirshner 1996; Riess et

al. 1998; Perlmutter et al. 1995, 1999). A correction factor can be applied to the peak magnitude to calibrate SNe Ia as standard candles. The intrinsic scatter in peak magnitudes and the differences in light curve shapes may cause a scatter in the visibility times of SNe, since brighter and broader SNe will have longer visibility times.

Perlmutter et al. (1999) show the distribution of correction factors (their Fig. 4). In order to account for this distribution, we have calculated the effective visibility times for SNe with various peak magnitudes and light-curve shapes. We then average these times using the distribution of peak magnitudes given by Perlmutter et al. (1999) as a weighting function. We thus obtain a function  $T(z, R_{lim})$  that fits a population of SNe Ia with properties similar to those observed by the SCP.

Having determined  $T(z, R_{lim})$  for a particular survey, we can calculate the redshift distribution of SNe Ia,  $N(z)$ , as a function of the model parameters. Figure 1d illustrates  $N(z)$  for the two examples of  $n(z)$  in Figure 1c. We then convert these redshift distributions to cumulative form, and

**Table 1.** The SCP SN sample

SN	Redshift
1997el	0.636
1997em	0.460
1997ep	0.462
1997eq	0.538
1997er	0.466
1997et	0.633
1997eu	0.592
1997ex	0.361
1997ey	0.575
1997ez	0.778
1997fa	0.498

use the Kolmogorov-Smirnov (KS) statistic to test if a data set is consistent with the predictions of a specific model. Figure 1 (panels e-f) shows an example of this procedure. Bloom (2003) presents a similar treatment of the redshift distribution of gamma-ray bursts.

### 3 APPLICATION TO AN OBSERVED SAMPLE OF HIGH-Z SUPERNOVAE IA

We now choose a sample of SNe Ia whose redshift distribution can be compared with predictions. Over the last few years, hundreds of high- $z$  SNe Ia have been discovered, mainly by the SCP (Perlmutter et al. 1995) and the High- $z$  Supernova Search Team (Schmidt et al. 1998). These SNe were discovered during numerous observing runs, using different telescopes and detectors, through various pass-bands and under non-uniform conditions. Given a complete description of the observations, a combined analysis of all available data sets should be feasible. At present, we limit ourselves to an analysis of a single data set obtained with a uniform observational setup, and for which most of the observational details are available, in particular estimates of the survey efficiency  $\eta$ .

The SCP have published the results of their efficiency studies for several SN samples (Pain et al. 2002). Here, we study the deepest and largest of these data sets. This SN sample is denoted as set ‘‘D’’ in the analysis of Pain et al. (2002). Following is a brief outline of the search procedure used to discover these SNe. Deep (3600 s, total)  $R$ -band exposures were obtained with the BTC camera mounted on the 4m Blanco telescope at CTIO, on December 28-29, 1997. These were compared with similar images obtained 36-37 days earlier. Seventeen candidate SNe were discovered, with discovery magnitudes  $21.6 < R < 24.5$  and redshifts  $0.36 < z < 0.86$ . Twelve SNe were spectroscopically confirmed as SNe Ia. However, only eleven of these were retained in the ‘‘statistical sample’’ used by Pain et al. (2002) to calculate SN rates, and these constitute the sample we analyze, presented in Table 1.

The SN sample was discovered in 11 different fields (Pain et al. 2002) observed under non-uniform atmospheric conditions, leading to survey efficiency curves  $\eta(R)$  which vary from field to field. We have averaged the efficiency curves measured for each field (kindly provided by R. Pain), to get the mean efficiency of the survey,  $\eta(R)$  (Figure 2).

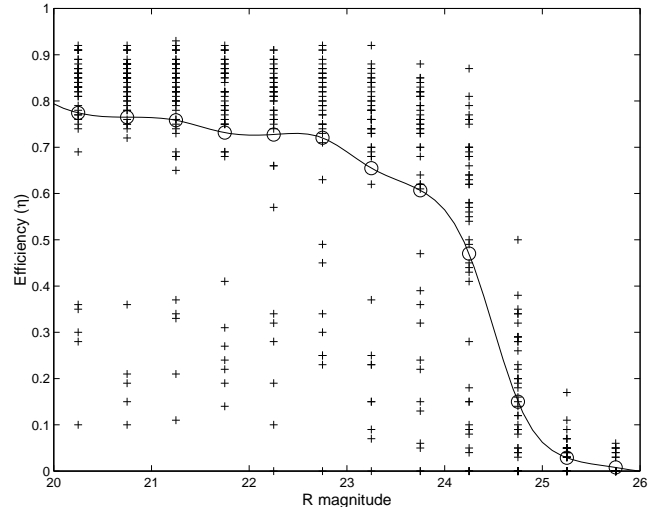


**Figure 2.** The mean efficiency of the SCP SN search described in § 3 as a function of  $R$ -band magnitude. Measurements of the detection efficiency in individual fields, kindly supplied by R. Pain, are given by + signs, while the open circles show the mean values. The solid curve is a cubic spline fit to the mean points, and is used in our calculation. Note the large vertical dispersion resulting from non-uniform atmospheric conditions and from the variable fraction of each field that was not used due to the presence of bright stars or other defects.

Since the efficiency enters our calculations in a linear fashion, calculating the SN redshift distribution using the mean curve is equivalent to performing the calculation for each field individually (with the appropriate efficiency curve) and summing the results. We neglect a possible redshift dependence of the efficiency due to the variation in the contrast between SN light and underlying host galaxy emission within a constant aperture. This contrast is reduced with redshift  $\propto D_L^{-2} (1+z)^4$ , where  $D_L$  is the luminosity distance. For our chosen cosmology, this gives a factor of  $\sim 3$  between  $z = 0.3$  and  $z = 1$ . Galaxy and SN K-corrections will offset some of this effect, and, from Fig. 2b of Pain et al. (2002) we can estimate that the remaining correction to the SN detection efficiency will be of a few per cent at most.

The search strategy employed by the observers in a certain survey can also influence the predicted redshift distribution of SNe Ia. In particular, the SCP survey whose data we use here requires that a candidate SN be brighter in a search image than in a reference image taken a few weeks earlier. This criterion was designed to discover only SNe near peak magnitude, and is driven by the SCP’s scientific goals (Perlmutter 1999, and references therein). The search criterion has implications for the calculation of the effective visibility times  $T(z)$ . For example, low- $z$  SNe, that are much brighter than the survey’s limiting magnitude  $R_{lim}$ , could, in principle, contribute significantly to  $T$  (Eq. 8). However, during most of the time these objects spend above  $R_{lim}$ , they are declining in magnitude, and therefore would have been ignored by the SCP. We therefore limit the calculation of  $T(z)$  to the period during which a SN is brighter in the second epoch image than it was 36 days before, when the reference images were obtained. This is achieved by multiplying the integrand in Eq. 8 by

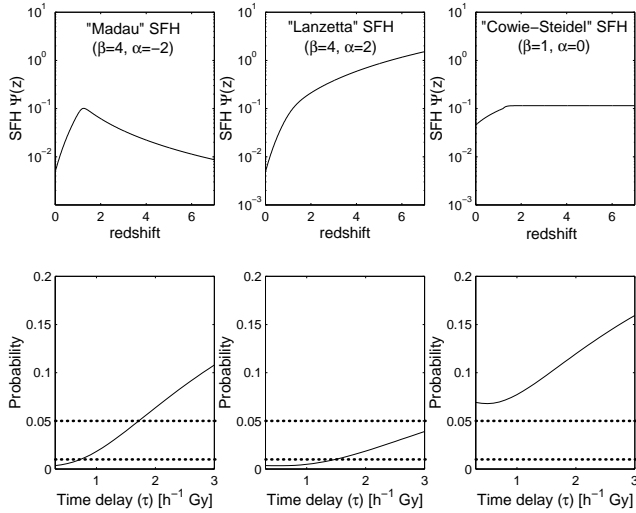


**Figure 3.** Probability of SN Ia time delay values, given the data, for particular SFH models. Assuming the SFH models shown in the upper panels, we can constrain the allowed values of  $\tau$  by the probability derived from the KS test (lower panels). Points below the upper and lower dotted lines are ruled out at 95% and 99% confidence, respectively.

$$S[R(t)] = \begin{cases} 1 & R(t) < R(t-36d) \\ 0 & R(t) \geq R(t-36d) \end{cases} \quad (9)$$

## 4 RESULTS

### 4.1 Star formation history and the delay time of SNe Ia

We have calculated the expected redshift distribution of SNe Ia for the above survey, for a range of characteristic delay times  $0.3 \leq \tau \leq 3 h^{-1}$  Gyr, and SFH indices  $-2 \leq \alpha \leq 2$  and  $1 \leq \beta \leq 4$ . Examination of the full range of models calculated shows that the data cannot constrain the model parameters individually, i.e., the characteristic delay time is degenerate with the SFH functional form. However, if we assume some prior, either on the time delay  $\tau$  or on the SFH, the data can be used to constrain the other parameters. For instance, Figure 3 shows the range of allowed values for  $\tau$  assuming some of the SFH functions appearing in the recent literature. We can see that if the Madau et al. (1998) SFH is assumed, the delay time  $\tau$  is constrained to be  $\tau \geq 1.7(\tau \geq 0.7)h^{-1}$  Gyr at the 95%(99%) confidence level (CL). Rising SFHs, similar to those advocated by Lanzetta et al. (2002), are ruled out at the 95% CL, unless  $\tau > 3h^{-1}$  Gyr. A gentler evolution of the SFH, e.g. as proposed by Cowie et al. (1999) and Steidel et al. (1999), places no constraints on  $\tau$ . Inspecting the actual distributions predicted by the various models (e.g., Fig. 1e and 1f), we find that invariably, the models that are ruled out by the data under-predict the number of SNe Ia at intermediate redshifts ( $z \sim 0.5$ ) relative to the number of SNe Ia at higher redshifts ( $z \sim 0.8$ ).

Figure 4 shows the constraints set on the SFH for given values of the delay time  $\tau$ . The first two panels show that, for short delay times ( $\tau < 0.5h^{-1}$  Gyr), the data constrain only the low- $z$  index  $\beta$ . For such short delays, the SFH at high  $z$  does not strongly affect (and is therefore not constrained

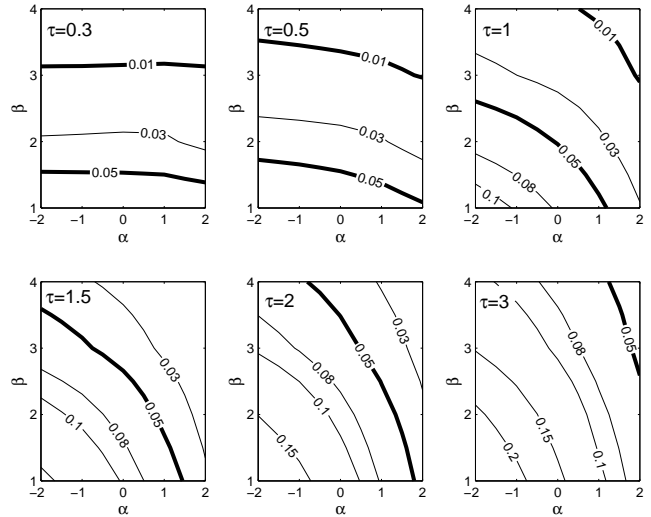


**Figure 4.** Constraints on SFH models for a given SN-Ia delay time. Each panel shows contours of equal probability, derived from the KS test for various combinations of the SFH indices  $\alpha$  and  $\beta$ , for the indicated SN Ia delay time,  $\tau$ , in units of  $h^{-1}$  Gyr.

by) the SN redshift distribution we measure at  $z < 1$ . If we assume such short time delays, the SN data require a gentle decline in SFH from  $z = 1$  to  $z = 0$  ( $\beta = 1$ ), favoring the results of Cowie et al. (1999) and Sullivan et al. (2000a) over those of Lilly et al. (1996) or the recent findings of Hippelein et al. (2003).

As we consider longer time delays ( $1 \leq \tau \leq 2h^{-1}$  Gyr), the data begin to constrain also the high- $z$  evolution of the SFH, parameterised by the index  $\alpha$ . Generally speaking, SFHs that decline above  $z = 1.2$  (e.g., Madau et al. 1998) are favored over the strongly rising functions of Lanzetta et al. (2002). For instance, a model where the SFH is rising at all  $z$  as  $\Psi \sim (1+z)^2$  (i.e.,  $\alpha = \beta = 2$ ) is ruled out at the 95% CL for time delays  $\tau \leq 2h^{-1}$  Gyr. The constraints are weakest when a long delay time,  $\tau = 3h^{-1}$  Gyr, is considered, in which case only SFH models combining a sharp increase at low redshift ( $\beta > 2$ ) that continues to rise steeply at high redshifts ( $\alpha = 2$ ) are ruled out at the 95% CL, and are thus disfavored by the data regardless of  $\tau$ . In conclusion, even with a small sample of 11 SNe Ia, it appears that the SN Ia redshift distribution can be used to set interesting limits on the SFH and the characteristic delay time of SNe Ia.

### 4.2 Caveats

We now consider possible caveats that might relax the constraints we have found. These may be due to some weakness in the model we have employed, or to effects related to the data set we have used. We discuss both possibilities below.

Our model includes two main parameterised components – the SFH and the SN Ia delay function. Our treatment of the SFH is fairly robust, since our parameterization covers the entire range of SFH functions reported in the literature. As for the SN Ia delay function, if SNe Ia are descended from a single or dominant type of progenitor, it will be reasonable to assume that there is a characteristic time delay between the formation of these systems and the SN explosion. Our parameterised models qualitatively reproduce the



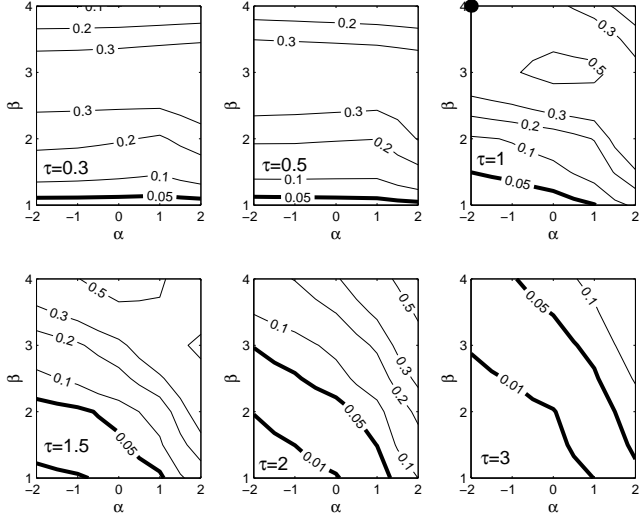


**Figure 6.** As in Fig. 4, but for a simulated data sample of 100 SNe, drawn from the distribution calculated for  $\alpha = -2$ ,  $\beta = 4$  and  $\tau = 1h^{-1}$  Gyr and assuming a survey with limiting magnitude  $R = 24$ . Note that the input model (marked with a filled circle) is recovered, and that significant areas of the parameter space are ruled out. However, individual limits either on the SFH indices ( $\alpha$  and  $\beta$ ) or the delay time  $\tau$  cannot be drawn.

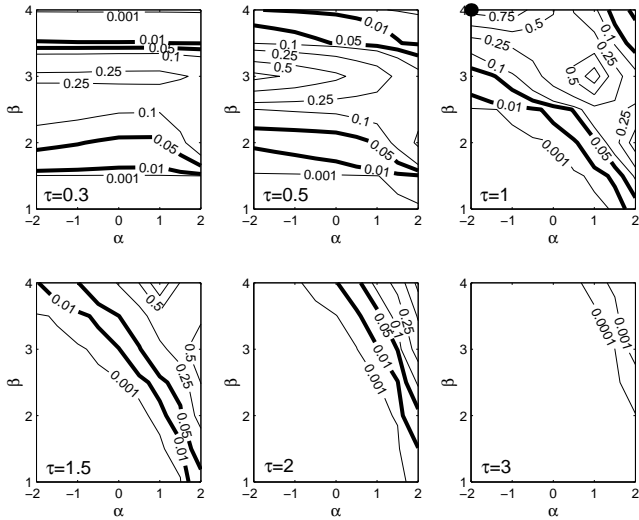


**Figure 7.** Similar to Fig. 6, but using a simulated sample of 1000 SNe to a limiting magnitude  $R = 25$ . Such a large data set could constrain both the SFH ( $\beta > 1$  at the 95% CL) and the SN Ia delay time ( $\tau < 3h^{-1}$  Gyr) simultaneously.

SNAP (Perlmutter et al. 2002) and the LSST (Strauss et al. 2002).

Figure 6 shows results of the first simulation. A data set of 100 SNe reaching  $R = 24$  mag should be a powerful tool to test the SFH and SN Ia delay times. While the input model ( $\alpha = -2, \beta = 4, \tau = 1$ ) is consistent with the data ( $P=0.49$ ), significant portions of the parameter space are ruled out. However, the degeneracy between the SFH indices  $\alpha$  and  $\beta$ , and the SN Ia delay time  $\tau$  persists, and the data cannot constrain each parameter individually.

Figure 7 shows the constraints that can be drawn from the larger, deeper sample. The “correct” model ( $\alpha = -2, \beta = 4, \tau = 1$ ) is recovered with a probability value of  $P = 0.79$ . Note that the degeneracy between the form of the SFH and the SN Ia delay time is now broken. Shallow SFHs at low  $z$  ( $\beta = 1$ ) and long delay times ( $\tau = 3$ ) are strongly ruled out by the data. Shorter delay times set strong constraints on the allowed values of the SFH indices  $\alpha$  and  $\beta$ .

## 5 DISCUSSION AND CONCLUSIONS

We have calculated the expected redshift distribution of SNe Ia in a magnitude limited survey for a wide set of model parameters, and compared our calculations with observations of high- $z$  SNe by the SCP. We have shown that this approach is significantly more powerful than comparing expected and observed SN rates, because of the redshift binning involved in deriving SN Ia rates. We confirm and quantify the findings of Pain et al. (2002) and Tonry et al. (2003) which suggest that the redshift distribution of SNe Ia at  $z \sim 0 - 1$  disfavor a strong variation of the SN Ia rate during this period. Thus, if the SFH between  $z = 0$  and 1 is steeper than  $\Psi \propto (1+z)$ , the delay time of SNe Ia must be long ( $\tau > 0.5h^{-1}$  Gyr). We show that, even for longer delay times ( $\tau \geq 1h^{-1}$  Gyr), the data set interesting constraints on the SFH. Generally, strongly rising SFHs, similar to those advocated by Lanzetta et al. (2002), fit the data poorly, and SFH models which rise steeply at low redshifts ( $\beta > 2$ ) and continue to rise at high redshifts ( $\alpha = 2$ ) are ruled out by the data at the 95% CL, unless  $\tau > 3h^{-1}$  Gyr. Turning the argument around, given some determinations of the SFH (e.g., Madau et al. 1998), we can constrain the characteristic delay time of SNe Ia to be  $\tau > 1.7h^{-1}$  Gyr ( $\tau > 0.7h^{-1}$  Gyr) at the 95%(99%) CL.

As already noted, Yungelson & Livio (2000) have studied the delay functions of different SNe Ia progenitor systems. In their double-degenerate (DD) model, two WDs merge, with the resulting WD reaching (or surpassing) the Chandrasekhar mass. Single degenerate models include accretion of He-rich material from a non-degenerate companion, leading to helium ignition on the WD surface and an edge-lit detonation (He-ELD). Alternatively, H-rich material from a main sequence companion is accreted and processed on the WD surface, and results either in an edge-lit detonation due to accumulated helium (MS-ELD) or to central carbon ignition as the WD reaches the Chandrasekhar mass (MS-CH).

The delay functions calculated for these models are more complex than the parameterised MDP forms we have used, but generic similarities exist. In particular, both DD and He-ELD curves can be characterised by a fast onset of SNe Ia, some  $3 \times 10^7$  years after star formation, followed by gradual increase and a decline that terminates in a sharp, exponential cutoff after  $\sim 1$  Gyr for the He-ELD and  $\sim 11$  Gyr for the DD models. This is qualitatively similar to the MDP exponential formulation we use. The MS-CH model can be approximated by a DF-like model with a delay time of  $\sim 1$  Gyr, so can be constrained by our calculation using this parameterization (§ 4.2, Figure 5). The MS-ELD is more complex, with a delayed onset of SNe Ia, about 0.3 Gyr af-

ter star formation, followed by an approximately power-law decline lasting some 11 Gyr.

If we consider those SFH determinations requiring long time delays in our models (e.g., Madau et al. 1998; Lanzetta et al. 2002), then the data disfavor the MS-CH and He-ELD progenitor models. We have shown that larger samples of SNe Ia, that will be obtained by future SN search programs, some of which are already in progress, could be used to obtain even stronger constraints on the SFH and SN Ia models.

In a companion paper (Maoz & Gal-Yam 2003), we study the implications of the measured SN Ia rates in  $z \sim 1$  galaxy clusters on the nature of SN Ia progenitors and the source of iron in clusters. We demonstrate there that, if SNe Ia have produced most of the iron in galaxy clusters, and the stars in clusters formed at  $z \sim 2$ , then the SN Ia delay time must be *lower* than 2 Gyr. Thus, if both conditions were met, then the Lanzetta et al. (2002) SFH would be ruled out by the data presented here.

Finally, it is interesting to note here that most previous authors have considered core-collapse SNe, whose rates closely track the SFH, as promising indicators for SFH measurement (but see DF 1999 for an alternative view). In principle, our methods could easily be applied also to high- $z$  core-collapse SN samples, if and when they become available. However, recent work by Mannucci et al. (2003) has shown that the majority of core-collapse events in star-forming galaxies suffers from strong dust extinction. SFH measurements using core-collapse SNe thus share the same problems that make UV-determined SFHs so widely debated – the strong dependence of the derived SFH on the little known amount and properties of dust at high redshifts. In contrast, most SNe Ia probably occur in relatively dust-free environments. Thus, measurements of the SFH using SNe Ia, through methods similar to the ones we have discussed here, may provide an attractive alternative to SFHs based on UV and emission line fluxes.

## ACKNOWLEDGMENTS

We thankfully acknowledge help, advice and fruitful discussions with R. Pain, T. Dahlén, P. Madau, C. Porciani, S. Fabbro, S. Perlmutter, B. Leibundgut, A. Filippenko, B. Schmidt, E. Ofek, O. Gnat, D. Poznanski and K. Sharon. This work was supported by the Israel Science Foundation — the Jack Adler Foundation for Space Research, Grant 63/01-1.

## REFERENCES

- Beuermann, K. et al. 1999, A&A, 352, L26  
 Bersier, D. et al. 2003, ApJL, 584, L43  
 Bloom, J. S. 2003, AJ, Submitted, astro-ph/0302249  
 Branch, D. 1998, ARA&A, 36, 17  
 Calura F. & Matteucci F., 2003, ApJ, in press, astro-ph/0307014  
 Connolly, A. J., Szalay, A. S., Dickinson, M., Subbarao, M. U., & Brunner, R. J. 1997, ApJL, 486, L11  
 Cowie, L. L., Songaila, A., & Barger, A. J. 1999, AJ, 118, 603  
 Dahlén, T., & Fransson, C. 1999, A&A, 350, 349 (DF)  
 Della Valle, M. & Livio, M. 1994, ApJL, 423, L31  
 Filippenko, A. V. 1997, ARA&A, 35, 309  
 Gal-Yam, A., Maoz, D., & Sharon, K. 2002, MNRAS, 332, 37  
 Garnavich, P. M. et al. 2002, BAAS, 201, 7809  
 Goldhaber, G., et al. 1997, in *Thermonuclear Supernovae* eds. P. Ruiz-Lapuente, R. Canal, & J. Isren (Dordrecht: Kluwer), P. 777  
 Hamuy, M., Phillips, M. M., Maza, J., Suntzeff, N. B., Schommer, R. A., & Aviles, R. 1995, AJ, 109, 1  
 Hamuy, M., Phillips, M. M., Suntzeff, N. B., Schommer, R. A., Maza, J., & Aviles, R. 1996, AJ, 112, 2391  
 Hardin, D. et al. 2000, A&A, 362, 419  
 Hippelein, H., et al. 2003, A&A, in press, astro-ph/0302116  
 Howell, D. A. 2001, ApJL, 554, L193  
 Jørgensen, H. E., et al. 1997, ApJ, 486, 110  
 Kobayashi, C., Tsujimoto, T., Nomoto, K., Hachisu, I., & Kato, M. 1998, ApJL, 503, L155  
 Kobayashi, C., Tsujimoto, T., & Nomoto, K. 2000, ApJ, 539, 26  
 Kolatt, T. S. & Bartelmann, M. 1998, MNRAS, 296, 763  
 Lanzetta, K. M., Yahata, N., Pascarelle, S., Chen, H., & Fernández-Soto, A. 2002, ApJ, 570, 492  
 Leibundgut, B., et al. 1996, ApJ, 466, 21  
 Li, W., Filippenko, A. V., Treffers, R. R., Riess, A. G., Hu, J., & Qiu, Y. 2001, ApJ, 546, 734  
 Lilly, S. J., Le Fevre, O., Hammer, F., & Crampton, D. 1996, ApJL, 460, L1  
 Madau, P., Ferguson, H. C., Dickinson, M. E., Giavalisco, M., Steidel, C. C., & Fruchter, A. 1996, MNRAS, 283, 1388  
 Madau, P., Della Valle, M., & Panagia, N. 1998 (MDP), MNRAS, 297, L17  
 Madau, P., Pozzetti, L., & Dickinson, M. 1998, ApJ, 498, 106  
 Mannucci, F. et al. 2003, A&A, 401, 519  
 Nugent, P., et al. 1998, IAUC 6804  
 Pain, R., et al. 1997, ApJ 473, 356  
 Pain, R. et al. 2002, ApJ, 577, 120  
 Pain, R. & SNLS Collaboration 2002, BAAS, 201, 4302  
 Perlmutter, S., et al. 1995, ApJ, 440, 41  
 Perlmutter, S., et al. 1998, Nature, 391, 51  
 Perlmutter, S., et al. 1999, ApJ, 517, 565  
 Perlmutter, S. & SNAP Collaboration 2002, BAAS, 201, 12602  
 Phillips, M. M. 1993, ApJ, L105, 413  
 Phillips, M. M. et al. 1999, AJ, 118, 1766  
 Riess, A. G., Press, W. H., & Kirshner, R. P. 1996, ApJ, 473, 88  
 Riess, A. G. et al. 1997, AJ, 114, 722  
 Riess, A. G., et al. 1998, AJ, 116, 1009  
 Riess, A. G. et al. 1999, AJ, 117, 707  
 Riess, A. G. et al. 2001, ApJ, 560, 49  
 Ruiz-Lapuente, P., & Canal, R. 1998, ApJ, 497, L57  
 Sadat, R., Blanchard, A., Guiderdoni, B., & Silk, J. 1998, A&A, 331, L69  
 Salpeter, E.E. 1955, ApJ, 121, 161  
 Schmidt, B.P., et al. 1998, ApJ, 507, 46  
 Smith, R. C. et al. 2002, BAAS, 201, 7808  
 Steidel, C. C., Adelberger, K. L., Giavalisco, M., Dickinson, M., & Pettini, M. 1999, ApJ, 519, 1  
 Strauss, M. A. 2002, BAAS, 201, 3402  
 Sullivan, M., Treyer, M. A., Ellis, R. S., Bridges, T. J., Milliard, B., & Donas, J. 2000a, MNRAS, 312, 442  
 Sullivan, M., Ellis, R., Nugent, P., Smail, I., & Madau, P. 2000b, MNRAS, 319, 549  
 Tonry, J. L., et al. 2003, ApJ, in press, astro-ph/0305008  
 Yungelson, L., & Livio, M. 2000, ApJ, 528, 108